Available online at www.sciencedirect.com
SCIENCE DIRECT®
ELSEVIER
Earth and Planetary Science Letters 211 (2003) 97–110
EPSL
www.elsevier.com/locate/epsl

Grain size evolution and the rheology of ductile shear zones: from laboratory experiments to postseismic creep

Laurent G.J. Montési *, Greg Hirth

Woods Hole Oceanographic Institution, Department of Geology and Geophysics, Woods Hole, MA 02543, USA

Received 15 November 2002; received in revised form 27 March 2003; accepted 2 April 2003

Abstract

Geologic, experimental, and geodetic studies indicate that ductile shear zones do not deform in steady state. We present a theoretical model for an elastically loaded ductile shear zone deforming by combined dislocation and diffusion creep, in which grain size is allowed to evolve toward its equilibrium (recrystallized) value. Several grain size evolution laws are considered. Simulations of laboratory experiments show that grain size evolution can lead to changes in the dominant deformation mechanism that are accompanied by transient strain-weakening or strain-strengthening episodes reminiscent of laboratory observations. Ductile shear zones can also produce postseismic creep as observed in geodetic data following large earthquakes. Non-steady-state ductile creep is difficult to differentiate from frictional sliding with velocity-strengthening friction. Hence, ductile creep may play a role in the transition from velocity-weakening to velocity-strengthening friction with increasing temperature.

Keywords: ductile creep; grain size evolution; transient creep; postseismic creep; friction laws

1. Introduction

At depths larger than a few kilometers, rocks are hot enough to flow by ductile creep, accommodated by motion of dislocations or diffusion of vacancies [1,2]. By definition, ductile behavior indicates that deformation remains distributed, in contrast to brittle behavior, for which deformation localizes on shear bands [3,4]. In the ductile regime, rocks are strain rate-hardening, which stabilizes deformation and impedes localization. However, localized shear zones are common in natural rocks that deformed by dislocation or diffusion creep [5]. Localization may be promoted by feedback loops involving temperature or grain size that lead to strain weakening [6–8]. Localization in the ductile regime is therefore transient, associated with a change in temperature or microstructure. Geological evidence supports the hypothesis that ductile shear zones are transient phenomena [9,10].

Strain weakening resulting from shear heating might cause strain localization in the ductile regime [9,11,12]. However, thermal effects alone are insufficient to cause strain localization unless deformation is already localized [8,13,14]. Indeed,

* Corresponding author. Tel.: +1-508-289-3708; Fax: +1-508-457-2187.
E-mail addresses: montesi@whoi.edu (L.G.J. Montési), ghirth@whoi.edu (G. Hirth).

0012-821X/03/$ – see front matter © 2003 Elsevier Science B.V. All rights reserved.
doi:10.1016/S0012-821X(03)00196-1

there is only scant evidence for a thermal anomaly associated with ductile shear zones [15].

By contrast, grain size reduction is observed in natural ductile shear zones [16–23]. Recrystallization can weaken the rock by producing small grains, which enhances diffusion creep, and by reducing the dislocation density. Laboratory samples deformed to large strain document recrystallization-induced weakening [24–31]. These experiments may be direct analogues of the rheological evolution of a ductile shear zone. We present a model for ductile shear zones that includes the evolution of grain size, and investigate its rheological response to sudden changes of loading velocity.

In nature, there are several reasons why the grain size of a rock evolves. At low temperature, the grain size is reduced through brittle processes. At higher temperature, the competing processes of static grain growth and dynamic recrystallization operate. Small grains grow to reduce surface energy, while subgrain rotation and grain boundary bulging produce new small grains (dynamic recrystallization). Hence, the average grain size evolves towards an equilibrium value, D, for which the two phenomena balance one another.

If a sudden change of loading velocity, like the start of a laboratory experiment, induces microstructural and rheological evolution, it is possible that earthquakes, viewed also as sudden changes of loading velocity, produce a short-lived deformation episode on nearby ductile shear zones. Geodetic data show that large ($M_w \gtrsim 7.0$) earthquakes are followed by fast aseismic creep on a planar zone surrounding the rupture area [32–36]. The creeping plane has been interpreted as a fault plane with velocity-strengthening friction [37,38]. Alternatively, we propose that the creeping plane is a ductile shear zone undergoing a transient episode of enhanced creep triggered by the earthquake. We use our ductile shear zone model to show that an episode of enhanced creep can indeed follow an earthquake.

In this paper, we use several descriptions of grain size evolution to explore the transient behavior of ductile shear zones. Two types of simulations are presented that illustrate the rheological consequences of grain size evolution. The first simulations aim at reproducing laboratory experiments and produce strain–stress curves that display transient strain weakening or hardening. The second simulations investigate the response of a ductile shear to earthquake cycles and compare the behavior of the ductile shear zone model with velocity-strengthening friction.

2. Ductile shear zone model

2.1. Rheology

At sufficiently high temperature, rocks deform by the motion of intracrystalline defects. The motion of linear defects (dislocations) results macroscopically in dislocation creep, in which the strain rate, $\dot{\varepsilon}_D$, and the applied stress, σ, are related by a power law:

$$\dot{\varepsilon}_D = A_D \sigma^{n_D} \tag{1}$$

where $n_D \approx 3$–5 and A_D is a function of temperature, water content, oxygen fugacity, etc. As these quantities do not evolve in the simulations presented here, A_D is treated as a constant.

Deformation can also be accommodated by the diffusion of point defects, such as vacancies, through grain interiors or boundaries, resulting macroscopically in diffusion creep. The strain rate accommodated by diffusion creep, $\dot{\varepsilon}_G$, depends on the stress, but also depends on the grain size, d:

$$\dot{\varepsilon}_G = A_G d^{-m} \sigma^{n_G} \tag{2}$$

with $n_G = 1$, $m \approx 2$–3, and A_G a constant.

These deformation mechanisms are independent [1]. Thus, the total strain rate of a material deforming by dislocation and diffusion creep is:

$$\dot{\varepsilon} = \dot{\varepsilon}_D + \dot{\varepsilon}_G = A_D \sigma^{n_D} + A_G d^{-m} \sigma^{n_G} \tag{3}$$

For a given grain size d, the combined creep is dominated by dislocation creep at high stress and diffusion creep at low stress (Fig. 1). This behavior can be idealized as a transition from diffusion to dislocation creep at a critical stress [17,20,39]. ter Heege et al. [40] show that when a continuous distribution of grain size is taken into account, the coefficient A_G depends on the width of the grain

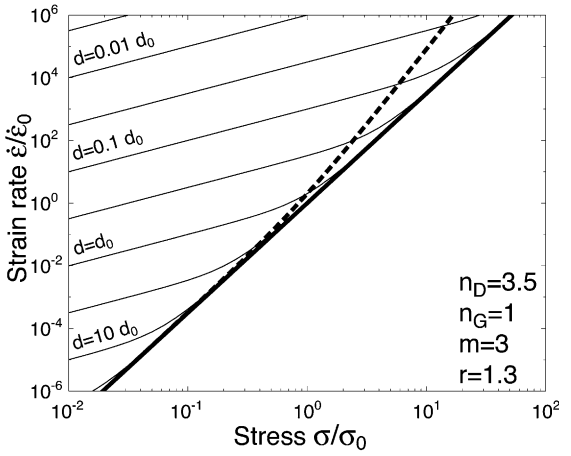

Fig. 1. Strain rate–stress curves for combined creep law for fixed grain size (thin solid lines), grain size at equilibrium (thick dashed line), and for a case with only dislocation creep (thick solid line). The scaling stress σ_0, strain rate $\dot{\varepsilon}_0$, and grain size d_0 are defined by Eqs. 20–22.

size distribution. Diffusion creep is enhanced if the grain size distribution is broader, which increases the critical stress for the transition from diffusion- to dislocation-dominated regimes.

Additional deformation mechanisms, such as low temperature plasticity, grain boundary sliding, or pressure solution, may also be included in Eq. 3. For simplicity, we restrict this study to the combined effect of dislocation and diffusion creep.

As already mentioned, the average grain size of a rock tends to evolve toward an equilibrium value, D. The equilibrium grain size depends on the stress, σ, as:

$$D = D_0 \sigma^{-r} \tag{4}$$

where D_0 and r are empirically determined constants [1]. If the grain size is at its equilibrium value (Eq. 4), the combined creep law becomes [8,41–43]:

$$\dot{\varepsilon} = A_D \sigma^{n_D} + A_G D_0^{-m} \sigma^{n_G + mr} \tag{5}$$

The values of $n_D = 3.5$, $m = 3$, and $r = 1.3$, published for dry olivine [39,44–46], result in $n_D < n_G + mr$. In this case, the combined creep at steady state is dominated by dislocation creep at low stress, where the equilibrium grain size is large and diffusion creep inefficient, and by diffusion creep at high stress, where the equilibrium grain size is small (Fig. 1). The relation between dislocation- and diffusion-dominated regimes is inverted compared to the case for a constant grain size d (Eq. 3). Hence, transient effects can arise as the dominant deformation mechanism changes when the grain size evolves from an initial value d_i to the equilibrium value D.

If the grain size obeys Eq. 4, the ratio of dislocation and diffusion creep depends on the applied stress. Alternatively, de Bresser et al. [47,48] reasoned that the equilibrium grain size is such that the ratio of dislocation- to diffusion-accommodated strain rate is a critical value, R, of order unity. They obtain:

$$D = (R A_G A_D^{-1})^{1/m} \sigma^{-(n_D - n_G)/m} \tag{6}$$

Substitution of Eq. 6 into Eq. 5 gives:

$$\dot{\varepsilon} = (1 + 1/R) A_D \sigma^{n_D} \tag{7}$$

2.2. Grain size evolution law

To fully characterize the deformation of a ductile rock, we need to know both the rheology for a given grain size (Eq. 3), and an equation that describes how the grain size evolves with time. In this study, we consider five grain size evolution laws. The first three laws are based on the competition between static grain growth and recrystallization, whereas the last two are ad hoc expressions for the evolution of grain size towards the equilibrium value D.

2.2.1. Field boundary law

Static grain growth is usually presented as a power law of time, $d^p - d_0^p = G(t - t_0)$, where G and p are constants and d_0 is the grain size at time t_0 [49]. This law can be recast as:

$$\dot{d} = G p^{-1} d^{1-p} \tag{8}$$

Dynamic recrystallization may be treated as a statistical phenomenon, where the probability of producing a new grain is higher for larger grains than small grains [43]. That probability also increases with the mobility of dislocations, approximated by the strain rate accommodated by dislo-

cation creep, $\dot{\varepsilon}_D$ [8,43]. Hence, the rate of decrease of the average grain size by dynamic recrystallization is proportional to $\dot{\varepsilon}_D$ and to the grain size, d [43]:

$$\dot{d} = -\dot{\varepsilon}_D d/\varepsilon_c \tag{9}$$

where the proportionality constant is expressed as ε_c, the critical strain for microstructural evolution. Experimental studies suggest that ε_c is of order unity [29,41,42].

de Bresser et al. [47,48] argue that dynamic recrystallization can be neglected in the diffusion-dominated regime, and that static grain growth does not operate in the dislocation-dominated regime. They propose that the boundary between these regimes occurs at a critical ratio of dislocation to diffusion creep, R. In this theory, called the field boundary theory of grain size evolution (FB), the grain size evolves following Eq. 8 if $\dot{\varepsilon}_D/\dot{\varepsilon}_G < R$ and following Eq. 9 if $\dot{\varepsilon}_D/\dot{\varepsilon}_G > R$:

$$\text{FB}: \dot{d} = \begin{cases} Gp^{-1}d^{1-p}, & \text{if } \dot{\varepsilon}_D/\dot{\varepsilon}_G < R \\ -\dot{\varepsilon}_D d/\varepsilon_c, & \text{if } \dot{\varepsilon}_D/\dot{\varepsilon}_G > R \end{cases} \tag{10}$$

In steady state, $\dot{\varepsilon}_D/\dot{\varepsilon}_G = R$, which results in Eqs. 6 and 7.

In the field boundary theory, it is assumed that the critical ratio, R, is a constant. As a result, the equilibrium grain size is different from Eq. 4. However, it is equally possible that R depend on stress. In particular, if $R = (A_D A_G^{-1} D_0^m)\sigma^{n_D - n_G - mr}$, the steady-state grain size relation follows Eq. 4. In this case, the boundary between dislocation- and diffusion-dominated regimes differs from that advocated by de Bresser et al. [47,48]. Expressing this boundary as a function of the grain size rather than the ratio of dislocation- and diffusion-induced strain rates, we obtain a modified field boundary theory (mFB):

$$\text{mFB}: \dot{d} = \begin{cases} Gp^{-1}d^{1-p}, & \text{if } d < D \\ -\dot{\varepsilon}_D d/\varepsilon_c, & \text{if } d > D \end{cases} \tag{11}$$

2.2.2. Continuous recrystallization law

The grain growth and recrystallization processes may not vanish when the critical ratio of dislocation to diffusion creep is reached. Hall and Parmentier [43] proposed to simply use the sum of these two processes in their continuous recrystallization grain size evolution law (CRX):

$$\text{CRX}: \dot{d} = \begin{cases} Gp^{-1}d^{1-p} - \dot{\varepsilon}_D d/\varepsilon_c \\ Gp^{-1}d^{1-p} - A_D\sigma^{n_D} d/\varepsilon_c \end{cases} \tag{12}$$

In this theory, the equilibrium grain size is defined by the condition that grain growth and recrystallization balance one another:

$$D = (A_D^{-1}\varepsilon_c G p^{-1})^{1/p}\sigma^{-n_D/p} \tag{13}$$

2.2.3. Grain size relaxation laws

Mathematically simpler grain size evolution laws leading to the steady-state grain size D have been proposed [8,41]. In these laws, the rate of grain size evolution is assumed to be proportional to the difference between the current grain size d and the equilibrium grain size D and to the strain rate. Kameyama et al. [41] and Braun et al. [42] use the total strain rate, whereas Montési and Zuber [8] include only the strain rate accommodated by dislocation creep, reasoning that recrystallization mechanisms involve the motion of dislocations. These assumptions lead respectively to the total rate relaxation (TRR) and dislocation rate relaxation (DRR) laws:

$$\text{TRR}: \dot{d} = \begin{cases} \dot{\varepsilon}(D-d)/\varepsilon_c \\ (A_D\sigma^{n_D} + A_G d^{-m}\sigma^{n_G}) \times (D_0\sigma^{-r} - d)/\varepsilon_c \end{cases} \tag{14}$$

$$\text{DRR}: \dot{d} = \begin{cases} \dot{\varepsilon}_D(D-d)/\varepsilon_c \\ A_D\sigma^{n_D}\ (D_0\sigma^{-r} - d)/\varepsilon_c \end{cases} \tag{15}$$

In the DRR model, an increase in grain size occurs only associated with dynamic recrystallization. Therefore, when $\dot{\varepsilon}_D \approx 0$, there is no grain growth. This aspect of the DRR model is unrealistic for single-phase aggregates, where grain growth is driven by a reduction in surface area and occurs even if the aggregate is not deforming. However, we suggest that the DRR model may be applicable for polyphase rocks, where static grain growth is impeded by secondary minerals [49].

2.2.4. Characteristics of the grain size evolution laws

Each of the five evolution laws (Eqs. 10, 11, 12, 14, and 15) predicts a specific relation between $\dot{d}$

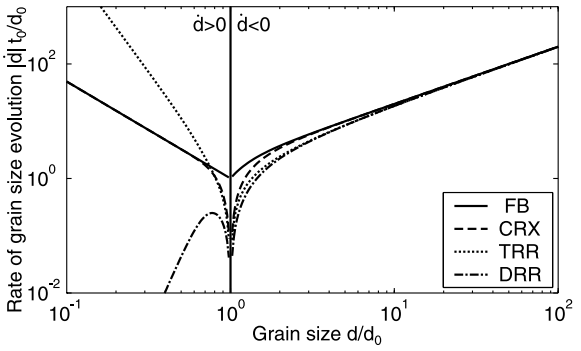

Fig. 2. Absolute value of the rate of grain size evolution as a function of current grain size at a strain rate of $\hat{\dot{\varepsilon}} = 1$, for which the FB and mFB models are identical. We use $\hat{G} = 1$. The grain size evolution rate is positive if $d < D$ and negative if $d > D$. Scaling described in Section 2.4.

and d, for a given strain rate (Fig. 2). The equilibrium grain size is defined as the grain size for which $\dot{d} = 0$. In the mFB, TRR, and DRR laws, the equilibrium grain size is specified a priori with Eq. 4. For the FB theory to give Eq. 4 at equilibrium, the critical ratio R must depend on stress, which gives the mFB theory. For the CRX theory to give Eq. 4 at equilibrium, the following relations must hold:

$$p = n_D / r \tag{16}$$

$$G = D_0^p A_D p / \varepsilon_c \tag{17}$$

For olivine, this implies $p \approx 2.7$ which is compatible with experimental results.

For a large grain size, all of the grain size evolution laws result in an exponential decay towards D. These laws are equivalent if $d \gg D$ (Fig. 2). When $d \ll D$, the FB, mFB, and CRX models predict rapid static grain growth. Eqs. 16 and 17 show that in the CRX theory, the rate of static grain growth is tied to the equilibrium grain size relation. By contrast, for the field boundary theories, the rate of static grain growth can be adjusted independently, without influencing the equilibrium grain size relation. The TRR law results in a rapid increase of grain size at small d, driven by the larger equilibrium value. While this resembles static grain growth, grain growth in the TRR law requires strain whereas static grain growth requires time. In the DRR law, grain growth requires dislocation creep and a small grain size. Hence, when the stress is low, as is the case when the grain size is small, the grains do not grow (Fig. 2). Therefore, the DRR law can represent conditions where static grain growth is inhibited by a secondary phase or fluids. While these conditions are not met in laboratory experiments on monomineralic rocks, they may be representative of natural conditions [50].

2.3. Loading system and shear zone simulations

For the simulations, we consider that a ductile shear zone is loaded elastically at a load point velocity V that can vary with time (Fig. 3). The stress changes at a rate proportional to the difference between the velocity across the shear zone, V_S, and the load point velocity, V:

$$\dot{\sigma} = K(V - V_S) \tag{18}$$

where K is the stiffness of the elastic coupling system.

If the shear zone has thickness H and deforms at strain rate $\dot{\varepsilon}$, $V_S = \dot{\varepsilon} H$. Then, using Eq. 3, we obtain an equation linking the rate of change of the stress to the current grain size and applied stress:

$$\dot{\sigma} = K[V - H(A_D \sigma^{n_D} + A_G d^{-m} \sigma^{n_G})] \tag{19}$$

The shear zone model is complete when an equation for the evolution of the grain size as a function of the applied stress and current grain size is chosen among Eqs. 10, 11, 12, 14, or 15. The resulting system of two equations is solved by

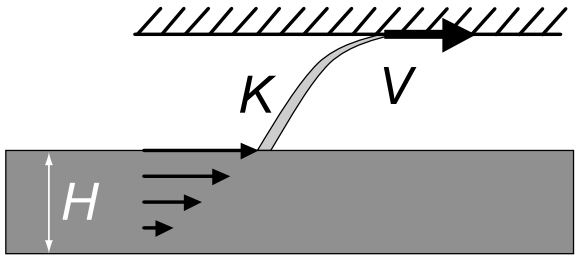

Fig. 3. Schematic representation of the shear zone model. A shear zone of thickness H and obeying the combined creep law and one of the grain size evolution law is loaded at velocity V through an elastic system of stiffness K.

a numerical Runge–Kutta method [51] for a given history of loading velocity $V(t)$ and initial conditions d_i and σ_i.

2.4. Scaling

All the simulations are conducted with the following non-dimensional quantities.

The first scale is the stress for which $\dot{\varepsilon}_D = \dot{\varepsilon}_G$, if the grain size is at equilibrium:

$$\sigma_0 = (A_D A_G^{-1} D_0^m)^{1/(n_G + mr - n_D)} \quad (20)$$

From the stress scale, we define the strain rate scale as the total strain rate in steady state at σ_0:

$$\dot{\varepsilon} = A_D \sigma_0^{n_D} + A_G D_0^{-m} \sigma_0^{n_G + mr} \quad (21)$$

and the grain size scale as the equilibrium grain size at σ_0:

$$d_0 = D_0 \sigma_0^{-r} \quad (22)$$

A natural time scale is that needed for evolution of the grain size by recrystallization at $\dot{\varepsilon}_0$:

$$t_0 = 2\varepsilon_c / \dot{\varepsilon}_0 \quad (23)$$

All non-dimensional quantities are denoted with a circumflex. With this scaling, the combined creep law becomes:

$$\hat{\dot{\varepsilon}} = (\hat{\sigma}^{n_D} + \hat{d}^{-m} \hat{\sigma}^{n_G})/2 \quad (24)$$

the equilibrium grain size is:

$$\hat{D} = \hat{\sigma}^{-r} \quad (25)$$

and the various grain size evolution laws are:

$$\text{TRR}: \quad \hat{\dot{d}} = (\hat{\sigma}^{n_D} + \hat{d}^{-m} \hat{\sigma}^{n_G})(\hat{\sigma}^{-r} - \hat{d}) \quad (26)$$

$$\text{DRR}: \quad \hat{\dot{d}} = \hat{\sigma}^{n_D} (\hat{\sigma}^{-r} - \hat{d}) \quad (27)$$

$$\text{CRX}: \quad \hat{\dot{d}} = \hat{d}^{1 - n_D/r} - \hat{\sigma}^{n_D} \hat{d} \quad (28)$$

$$\text{FB}: \quad \hat{\dot{d}} = \begin{cases} \hat{G} d^{1 - n_D/r}, \text{ if } \hat{d}^m \hat{\sigma}^{n_D - n_G} < R \\ -\hat{\sigma}^{n_D} \hat{d}, \text{ if } \hat{d}^m \hat{\sigma}^{n_D - n_G} > R \end{cases} \quad (29)$$

$$\text{mFB}: \quad \hat{\dot{d}} = \begin{cases} \hat{G} d^{1 - n_D/r}, \text{ if } \hat{d} < \hat{D} \\ -\hat{\sigma}^{n_D} \hat{d}, \text{ if } \hat{d} > \hat{D} \end{cases} \quad (30)$$

where $\hat{G} = G r t_0 / n_D d_0^p$ is a non-dimensional parameter describing the importance of static grain growth over dynamic recrystallization. For the CRX law, $\hat{G}$ is fixed to 1 because the equilibrium grain size is defined by a balance between recrystallization and static grain growth.

The stress evolution equation, which is derived from the elastic loading, becomes:

$$\hat{\dot{\sigma}} = \hat{K}[\hat{V} - (\hat{\sigma}^{n_D} + \hat{d}^{-m} \hat{\sigma}^{n_G})/2] \quad (31)$$

where $\hat{V} = V / H \dot{\varepsilon}_0$ and $\hat{K} = 2KH\varepsilon_c / \sigma_0$ are the non-dimensional load point velocity and stiffness of the loading system, respectively.

For all applications, we use $\hat{K} = 1$ and the parameters for olivine aggregates: $n_D = 3.5$, $n_G = 1$, $m = 3$, and $r = 1.3$. We verified that changing these parameters does not affect the general behavior presented below.

3. Simulation of laboratory experiments

In a simple laboratory experiment, a sample is loaded at constant velocity $\hat{V}$, with an initial grain size $\hat{d}_i$ and no initial stress. We conduct similar simulations, in which the initial stress is $\hat{\sigma}_i = 1/100 \sim 0$ and the initial grain size is not necessarily the steady-state value for the loading velocity. We first consider the response of a shear zone to simple shear loading and then compare it with laboratory experiments.

3.1. Simple shear experiments

Simple shear simulations are presented in Fig. 4, with different initial grain sizes, the same loading velocity $\hat{V} = 1$, and two different grain size evolution laws, DRR (Eq. 27) and CRX (Eq. 28. At steady state, we expect equal contributions from dislocation and diffusion creep, $\hat{\sigma} = 1$, and $\hat{d} = 1$.

If the initial grain size is large, the two grain size evolution laws result in similar stress–strain curves. Initially, the stress increases linearly with time as the shear zone is loaded elastically. At high enough stress, the shear zone deforms at a rate similar to the loading velocity. Creep is in quasi-steady state, but is dominated by dislocation creep, because the grain size is still large.

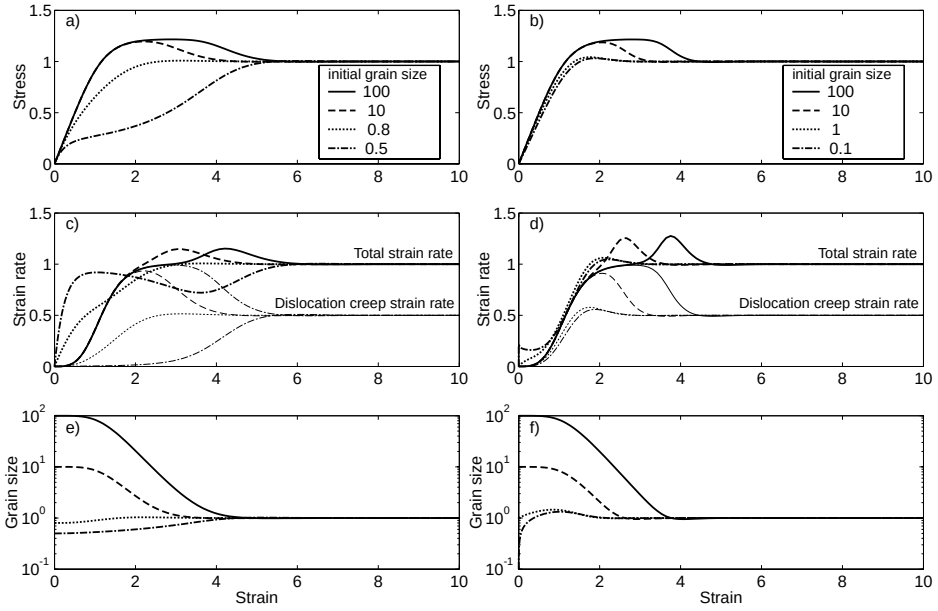

Fig. 4. Evolution of stress (a,), strain rate (c,d; thicker lines: total strain rate; thinner lines: strain rate by dislocation creep only), and grain size (e,f) for simulations of laboratory experiments with different grain size. The DRR grain size evolution law is used for a,c,e, and the CRX grain size evolution law is used for b,d,f.

Hence, the stress is higher than the steady-state value. During this period, the grain size decreases towards the equilibrium value. When the grain size is small enough for diffusion creep to be important, the shear zone displays strain weakening. The shear zone accelerates and deforms faster than it is loaded, relieving the stress. Finally, the shear zone reaches steady state.

If the initial grain size is small, the shear zone starts deforming at low stress in the diffusion-dominated regime. It then undergoes a period of strain hardening as the grain size increases towards the equilibrium value. There is no quasi-steady state before the strain-hardening period. However, if static grain growth is inhibited (i.e., using the law DRR) and the grain size is very small, the applied stress can be very small and grain size evolution extremely slow. If static grain growth is included, the initially small grain size increases quickly, even during the nominally elastic loading period (Fig. 4d). When the stress is sufficient for creep to occur, the grain size can be close to or even exceed the equilibrium value. In this case, there is no difference between the loading curves for any initial grain size smaller than the equilibrium value.

In Fig. 5, we present the stress–strain curves for different simulations with the same loading velocity $\hat{V}=1$, the same initial grain size $\hat{d}_i=0.5$, but different evolution laws. For the TRR and CRX laws, which have fast grain growth at small grain size (Fig. 2), the initial hardening is easily mistak-

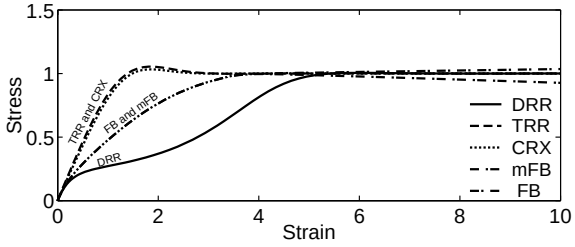

Fig. 5. Evolution of stress for shear zones obeying different grain size evolution laws with an initial grain size of $\hat{d}=0.5$, and loading velocity $\hat{V}=1$. $\hat{G}=0.1$ for the simulation using the mFB and FB laws.

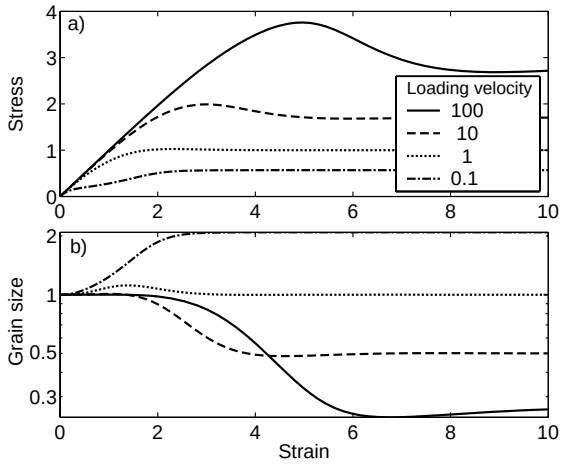

Fig. 6. Evolution of stress (a) and grain size (b) for a shear zone obeying the DRR grain size evolution law, an initial grain size of $\hat{d}=1$ and varying loading velocity.

en for elastic loading. For the DRR law, which does not include static grain growth, there is a much slower hardening rate. If $\hat{G}=1$ with the FB and mFB laws, static grain growth is fast and the simulation results are similar to the CRX case. With the FB and mFB laws, we can reduce the rate of static grain growth independently of the equilibrium grain size. By setting $\hat{G}$ at 0.1, we observe a behavior intermediate between the CRX ($\hat{G}=1$) and DRR ($\hat{G}=0$) simulations (Fig. 5).

In summary, the ductile shear zone model exhibits two types of responses to loading at a constant velocity: one with transient weakening, the other with transient hardening. The transition between these two types of responses is presented as a function of initial grain size in Fig. 4. The same transition occurs with changes in loading velocity (Fig. 6). If the loading velocity is high, dislocation creep is favored. The resulting stress–strain curve displays transient weakening, similar to the case with large initial grain size. If the loading velocity is low, which initially favors diffusion creep, we observe strain hardening as the grain size increases towards the steady-state value and diffusion creep becomes less important. As before, static grain growth mitigates this effect by producing large grains quickly.

3.2. Comparison with laboratory experiments

Several recent experiments on microstructural evolution display stress–strain curves similar to our simulations. As we use parameters relevant for dry olivine, our simulations are most readily compared with the experiments of Bystricky et al. [28]. In these experiments, the recrystallized grain size is about a factor of 10 smaller than the initial grain size. For these conditions, we predict an initial yield point about 20% higher than the final steady-state stress and no stress plateau as the sample recrystallizes, in agreement with experimental results.

With an initial grain size 10 times larger than the final grain size, as observed in Bystricky et al.'s experiments [28], the difference between simulations using alternative flow laws is minimal. To address which grain size evolution law is most applicable to these experiments, it will be important to consider the effect of velocity steps in which the loading velocity is suddenly reduced or increased. The grain size evolution laws also give very different results in situations where the grain size increases. Karato et al. [39] report on triaxial experiments on olivine with a variety of initial grain size, including some with small initial grain size. These experiments display hardening associated with grain growth, as in our simulations. An experiment in which deformation was interrupted showed time-dependent hardening, which is interpreted as evidence for static grain growth. This implies that laws like CRX or FB are more relevant in the laboratory for single-phase aggregates. The alternative laws, such as TRR and DRR, link grain growth to deformation of the sample, not time, and cannot replicate Karato et al.'s observations. However, in nature, static grain growth may be impeded by a pinning second phase [49] and a law for which small grains do not grow, such as DRR, may be applicable.

One difference between our simulations and the experiments is the shear zone geometry. Whereas we assume a simple shear geometry, the experiments are conducted in a rotary shear apparatus, in which the angular velocity of the shear zone is imposed, and the total torque on the sample is

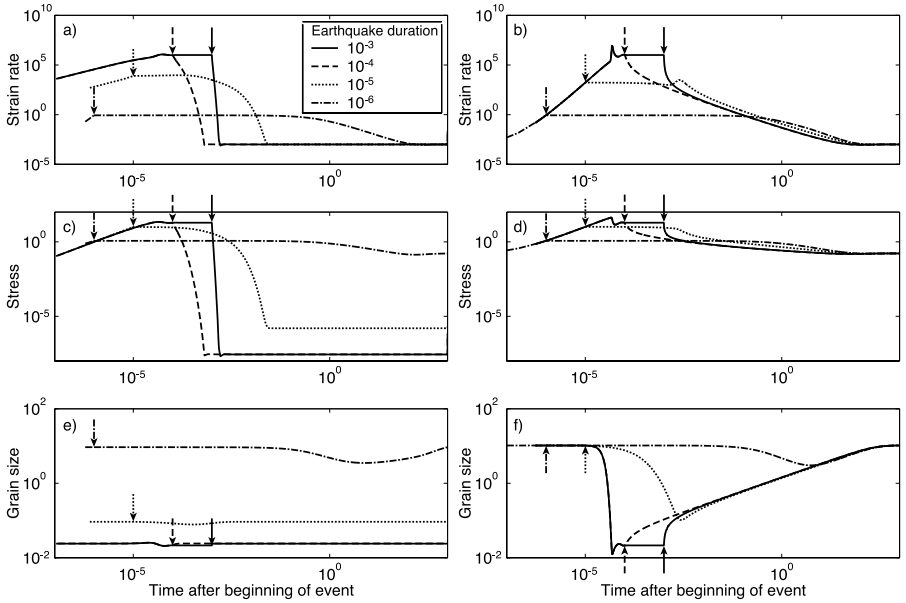

Fig. 7. Evolution of strain rate (a,b), stress (c,d), and grain size (e,f) for simulations of shear zone response to earthquake loading for different earthquake durations and using the DRR grain size evolution law (a,c,e) or the CRX grain size evolution law (b,d,f). The arrows indicate the end of the coseismic period for simulations with matching line style.

measured. The torque is an integration of the stress over the entire sample. At each location, the stress is a function of the local strain and strain rate, which depend on radius. We adapted our shear zone model for a rotary shear geometry. The resulting time–torque curves are similar to the simple shear results presented in Figs. 4–6.

4. Response to earthquakes

An earthquake may be seen as a short period of time during which shear displacement on a fault is much more rapid than during the intervening period. If a ductile shear zone is present in the vicinity of a seismogenic fault, for instance as an extension of the fault plane at depth, it will be loaded during an earthquake at a faster rate than during interseismic periods. We present simulations of the response of ductile shear zones to an earthquake-like loading.

We consider that earthquakes, of duration $\hat{T}_E$, occur periodically with a recurrence interval $\hat{T}_R \gg \hat{T}_E$. The loading velocity is $\hat{V}_{is}$ during the interseismic period and $\hat{V}_{cs}$ during the coseismic interval. In the simulations presented herein, we use $\hat{T}_R = 1000$, $\hat{V}_{is} = 10^{-6}$, and $\hat{V}_{cs} = 10^{3}$. The velocity jump of nine orders of magnitude between coseismic and interseismic displacement rates is similar to that experienced in nature. We vary $\hat{T}_E$ from 10^{-6} to 10^{-3}. The simulation is conducted for 20 earthquake cycles in order to reach a limit cycle, independent of initial conditions. We present only the last of these cycles in Fig. 7. We note that in most simulations, the limit cycle is reached at the second or third cycle.

If the earthquake lasts long enough, steady state is attained for the fast coseismic velocity (Fig. 7a). The grain size at the end of the earthquake is very small and tends to increase in the interseismic interval. However, in the absence of static grain growth (DRR law), the grain size is virtually unchanged during the interseismic period because of the low residual stress (Fig. 7c,e). Hence, the shear zone is able to deform at the coseismic rate during the next earthquake without requiring a large microstructural adjustment. However, by including grain growth (CRX law),

the grain size reaches the steady-state value at the interseismic velocity (Fig. 7f). The strength of the shear zone, when loaded at coseismic velocities, is very high. As a result, a slip deficit builds up during the earthquake, leading to prolonged creep after the earthquake ends. The rate of postseismic creep decreases approximately as a power law in time (Fig. 7b).

With short-duration earthquakes, steady state is not attained in the coseismic period, regardless of the grain size evolution law (Fig. 7). The grain size remains close to the large equilibrium value for interseismic velocities and the shear zone deforms for a significant portion of the interseismic interval at a rate intermediate between the coseismic and interseismic rates.

The periods of high strain rate that follow earthquakes in these simulations may be observed geodetically after large earthquakes. Such earthquakes are followed by a prolonged period of aseismic creep occurring mainly on the extension of the fault plane at depth [32–35]. Because of the higher temperatures at depth, it is possible that the extensions of the fault plane are ductile shear zones [52]. Hence, postseismic creep may be due to ductile creep triggered by the earthquake. More realistic simulations, including depth dependence of the shear zone parameters, elastic coupling, and slip complexity on the fault surface, must be conducted before this hypothesis can be tested.

5. Comparison with rate- and state-dependent friction

Postseismic creep may also be due to velocity-strengthening friction [37,38]. Indeed, frictional sliding becomes velocity-strengthening above a critical temperature, leading to a stably sliding deep fault plane [53–58]. One prediction of our model is a power law decay of the creep rate, which contrasts with the exponential decay predicted by velocity-strengthening friction. It is possible that geodetic data can differentiate between these models although recent numerical simulations of postseismic creep following the 1999 Izmit earthquake show that even very different assumptions about the deep fault behavior can produce similar creep patterns [38]. Next, we show how ductile creep can result in a behavior similar to that predicted by velocity-strengthening friction in typical laboratory experiments.

Rock friction can be described in the framework of rate- and state-dependent friction (RSDF) theory, whereby the coefficient of friction, μ, depends on the sliding velocity, V, and on a state variable θ, which is related to the microstructure of the sliding surface [59]. The state variable may evolve with time or slip towards a steady value that depends only on the current sliding velocity [60,61]. In RSDF theory, the shear stress on the fault is:

$$\tau = \sigma_n \mu = \tau_0 + A \ln (V/V_0) + B \ln (\theta V_0/D_C) \quad (32)$$

where σ_n is the normal stress on the fault, τ_0 and V_0 are reference values of the shear stress and the sliding velocity, and A, B, and D_C quantify the response of μ to a change in V at constant θ, the evolution of θ, and the critical distance for evolution of θ, respectively. At steady state, $\theta = D_C/V$, and the shear stress is:

$$\tau = \tau_0 + (A-B) \ln (V/V_0) \quad (33)$$

If $A-B<0$, the steady-state friction decreases with increasing velocity. The situation is unstable and may lead to earthquakes [62,63]. By contrast, when $A-B>0$, sliding is stable. In the laboratory, the transition to velocity strengthening may correspond to the onset of ductility in the rock [52,54]. The transition corresponds to the appearance of a second state variable with strongly positive $A-B$ and large D_C, which dominates the steady-state regime without eliminating the effects of the first state variable [57,58].

The second state variable may be a manifestation of ductile behavior in the fault gouge. The constitutive equations defined in Section 2 are a type of rate- and state-dependent rheology, for which the state variable is explicitly the grain size. The coefficients A and $A-B$ of the RSDF laws are most simply defined from the change of frictional resistance to an infinitesimal change of V at constant θ (i.e., constant d) and in steady

state (i.e., $d=D$), respectively. Velocity step experiments conducted on a ductile shear zone with evolving grain size give apparent values of A and $A-B$:

$$A=\begin{cases}\left.\dfrac{\partial\sigma}{\partial V}\right|_{d\ \text{constant}}\\ \sigma_0\dfrac{1+\hat{\sigma}^{n_G+mr-n_D}}{n_D+n_G\hat{\sigma}^{n_G+mr-n_D}}\end{cases} \tag{34}$$

$$A-B=\begin{cases}\left.\dfrac{\mathrm{d}\sigma}{\mathrm{d}V}\right|_{d=D}\\ \sigma_0\dfrac{1+\hat{\sigma}^{n_G+mr-n_D}}{n_D+(n_G+mr)\hat{\sigma}^{n_G+mr-n_D}}\end{cases} \tag{35}$$

where $\hat{\sigma}$ is the stress immediately before the velocity step. These relations are illustrated in Fig. 8. Note that $A-B$ is always positive, indicating that deformation is always stable in this model. Hence, ductile creep is inconsistent with RSDF at low temperature, where $A-B<0$.

The parameters A, B, and D_C (Eq. 32) are determined experimentally from the response of a fault to sudden changes in loading velocity. We simulate such experiments with our shear zone model and analyze them within the framework of RSDF laws (Fig. 9). In these simulations, the initial velocity is $\hat{V}=1$ and the shear zone is initially in steady state. At time zero, the velocity is increased (Fig. 9a) or decreased (Fig. 9b) by a factor of 10. The simulation is continued until

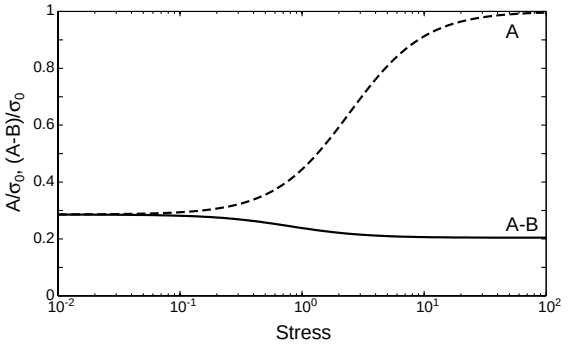

Fig. 8. Apparent rate- and state-dependent friction parameters $A-B$ (solid line) and A (dashed line) for a shear zone deforming by combined dislocation and diffusion creep with $n_D=3.5$, $n_G=1$, $m=3$, and $r=1.3$.

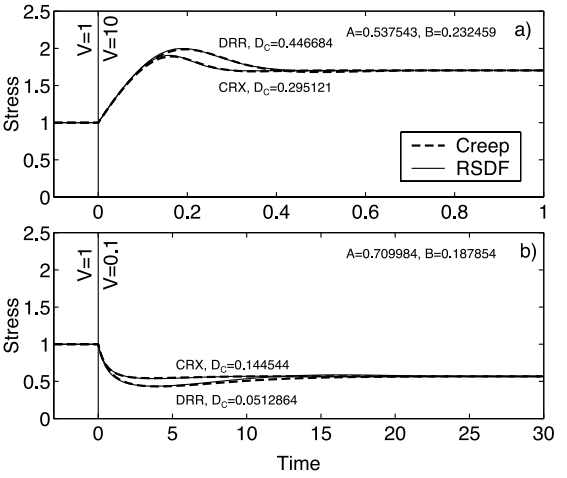

Fig. 9. Thick dashed lines: response of a shear zone deforming by combined diffusion and dislocation creep to (a) an increase or (b) a decrease of the loading velocity by a factor of 10. The curves are labelled by the grain size evolution law. Thin solid lines: Best-fitting simulation with rate- and state-dependent friction. In each case, the fit is virtually perfect.

the shear zone is at steady state for the final loading velocity. Then, we fit the stress–state curves with the RSDF formulation. In addition to Eq. 32, we need to define an evolution law for the state variable θ. We use the evolution law proposed by Dieterich [60]:

$$\mathrm{d}\theta/\mathrm{d}t=1-V\theta/D_C \tag{36}$$

Alternative state evolution laws give comparable results.

In our fitting algorithm, the parameters A and $A-B$ are determined a priori from Eqs. 34 and 35 modified for a finite change in loading velocity. The parameter D_C, however, cannot be specified a priori. Hence, we explore a large range of candidate values, and retain the value of D_C that produces the closest match to the ductile shear zone simulation.

In all cases, an almost perfect match can be found (Fig. 9). It would be impossible to differentiate experimentally between RSDF and ductile creep if only one of these stress–strain curves was available. However, during ductile creep, the values of A, B, and D_C inferred from the stress–strain curves change as a function of the magni-

tude and direction of the velocity step, with an increase of velocity yielding smaller A and $A-B$ and larger B and D_C values than a decrease of loading velocity. It may be possible to differentiate between the combined creep rheology and RSDF using relaxation experiments because the strain rate of the ductile shear zone cannot be lower than the dislocation creep rate, which depends on the applied stress only. By contrast, the frictional theory allows arbitrarily small velocity at a given stress.

6. Conclusions

We have presented a formulation for combined dislocation and diffusion creep that considers the evolution of grain size with time and/or deformation. Several grain size evolution laws were employed to explore the effects of static grain growth and dynamic recrystallization. The grain size evolution laws were included in a shear zone model to simulate the response of a ductile shear zone to sudden changes of loading velocity. The transitional effects observed in the simulations compare favorably with laboratory experiments on the effect of microstructural evolution on rock rheology. We also found that the ductile shear zone response resembles rate- and state-dependent friction. Simulations of the shear zone response to earthquake cycles predict episodes of enhanced creep following earthquakes, which are possible analogues of postseismic creep observed geodetically following major $M > 7.0$ earthquakes.

Acknowledgements

We thank Scott King and Norm Sleep for their comments on the manuscript. We are grateful to Chad Hall for sharing with us his insight on grain size evolution and pre-publication manuscripts. This work was supported by the Postdoctoral Scholar Program at the Woods Hole Oceanographic Institution, with funding provided by the USGS, by NSF Grant OCE-9907244 and a grant from the Deep Ocean Exploration Institute at WHOI. *[SK]*

References

[1] J.-P. Poirier, Creep of Crystals, Cambridge University Press, Cambridge, 1985.
[2] B. Evans, D.L. Kohlstedt, Rheology of rocks, in: T.J. Ahrens (Ed.), Rock Physics and Phase Relations: A Handbook of Physical Constants, AGU Reference Shelf, Vol. 3, Am. Geophys. Union, Washington, DC, 1995, pp. 148–165.
[3] D. Griggs, J. Handin, Observations on fracture and a hypothesis of earthquakes, in: D. Griggs, J. Handin (Eds.), Rock Deformation, Geol. Soc. Am. Mem. 79 (1960) 347–364.
[4] D.L. Kohlstedt, B. Evans, S.J. Mackwell, Strength of the lithosphere: Constraints imposed by laboratory experiments, J. Geophys. Res. 100 (1995) 17587–17602.
[5] J.G. Ramsay, Shear zone geometry, a review, J. Struct. Geol. 2 (1980) 83–99.
[6] J.-P. Poirier, Shear localization and shear instability in materials in the ductile field, J. Struct. Geol. 2 (1980) 135–142.
[7] B.E. Hobbs, H.-B. Mühlhaus, A. Ord, Instability, softening and localization of deformation, in: R.J. Knipe, E.H. Rutter (Eds.), Deformation Mechanisms, Rheology and Tectonics, Geol. Soc. London Spec. Publ. 54 (1990) 143–165.
[8] L.G.J. Montési, M.T. Zuber, A unified description of localization for application to large-scale tectonics, J. Geophys. Res. 107 (2002) 10.1029/2001JB000465.
[9] B.E. Hobbs, A. Ord, C. Teyssier, Earthquakes in the ductile regime?, Pure Appl. Geophys. 124 (1986) 309–336.
[10] J.-P. Burg, Ductile structures and instabilities: Their implications for Variscan tectonics in the Ardennes, Tectonophysics 309 (1999) 1–25.
[11] C. Froidevaux, G. Schubert, Plate motion and structure of the continental asthenosphere: A realistic model of the upper mantle, J. Geophys. Res. 80 (1975) 2553–2564.
[12] B.E. Hobbs, A. Ord, Plastic instabilities: Implications for the origin of intermediate and deep focus earthquakes, J. Geophys. Res. 93 (1988) 10521–10540.
[13] J.-P. Brun, P.R. Cobbold, Strain heating and thermal softening in continental shear zones: a review, J. Struct. Geol. 2 (1980) 149–158.
[14] L. Fleitout, C. Froidevaux, Thermal and mechanical evolution of shear zones, J. Struct. Geol. 2 (1980) 159–164.
[15] A. Camacho, I. McDougall, R. Armstrong, J. Braun, Evidence for shear heating, Musgrave Block, Central Australia, J. Struct. Geol. 23 (2001) 1007–1013.
[16] N.S. Mancktelow, Quartz textures from the Simplon Fault Zone, southwest Switzerland and north Italy, Tectonophysics 135 (1987) 133–153.
[17] E.H. Rutter, K.H. Brodie, The role of tectonic grain size reduction in the rheological stratification of the lithosphere, Geol. Rundsch. 77 (1988) 295–308.
[18] R.J. Knipe, Microstructural analysis and tectonic evolution in thrust systems: Examples from the Assynt region of the Moine Thrust Zone, Scotland, in: D.J. Barber,

P.G. Meredith (Eds.), Deformation Processes in Mineral, Ceramics, and Rocks, Unwin Hyman, London, 1990, pp. 228–261.
[19] J.D. Fitz Gerald, H. Stünitz, Deformation of granitoids at low metamorphic grade. I: Reactions and grain size reduction, Tectonophysics 221 (1993) 269–297.
[20] G.E. Jaroslow, G. Hirth, H.J.B. Dick, Abyssal peridotite mylonites: Implications for grain-size sensitive flow and strain localization in the oceanic lithosphere, Tectonophysics 256 (1996) 17–37.
[21] D. Jin, S.-I. Karato, M. Obata, Mechanisms of shear localization in the continental lithosphere: Inference from the deformation microstructures from the Ivrea zone, Northwest Italy, J. Struct. Geol. 20 (1998) 195–209.
[22] G. Molli, P. Conti, G. Giorgetti, M. Meccheri, N. Oesterling, Microfabric study on the deformational and thermal history of the Alpi Apuane marbles (Carrara marble), Italy, J. Struct. Geol. 22 (2000) 1809–1825.
[23] M. Bestmann, K. Kunze, A. Matthews, Evolution of calcite marble shear zone complex on Thassos Island, Greece: Microstructural and textural fabrics and their kinematic significance, J. Struct. Geol. 22 (2000) 1789–1807.
[24] J. Tullis, R.A. Yund, Dynamic recrystallization of feldspar: A mechanism for ductile shear zone formation, Geology 13 (1985) 238–241.
[25] J. Tullis, L. Dell'Angelo, R.A. Yund, Ductile shear zones from brittle precursors in feldspathic rocks: The role of dynamic recrystallization, in: A.G. Duba, W.B. Durham, J.W. Handin, H.F. Wang (Eds.), The Brittle-Ductile Transition in Rocks, AGU Geophys. Monogr. 56 (1990) 67–82.
[26] G. Hirth, J. Tullis, Dislocation creep regimes in quartz aggregates, J. Struct. Geol. 14 (1992) 145–159.
[27] E.H. Rutter, On the relationship between the formation of shear zones and the form of the flow law for rocks undergoing dynamic recrystallization, Tectonophysics 303 (1999) 147–158.
[28] M. Bystricky, K. Kunze, L. Burlini, J.-P. Burg, High shear strain of olivine aggregates: Rheological and seismic consequences, Science 290 (2000) 1564–1567.
[29] M. Pieri, L. Burlini, K. Kunze, I. Stretton, D.L. Olgaard, Rheological and microstructural evolution of Carrara marble with high shear strain: Results from high temperature torsion experiments, J. Struct. Geol. 23 (2001) 1393–1413.
[30] F. Heidelbach, I. Stretton, K. Kunze, Texture development of polycrystalline anhydrite experimentally deformed in torsion, Int. J. Earth Sci. 90 (2001) 118–126.
[31] E. Rybacki, M.S. Paterson, R. Wirth, G. Dresen, Rheology of calcite-quartz aggregates deformed to large strain in torsion, J. Geophys. Res. 108 (2003) 10.1029/2002JB001833.
[32] R. Bürgmann, P. Segall, M. Lisowski, J.L. Svarc, Postseismic strain following the Loma Prieta earthquake from repeated GPS measurements, in: The Loma Prieta, California, Earthquake of October 17, 1989 – Postseismic Effects, Aftershocks and Other Phenomena, U.S. Geol. Surv. Prof. Pap. 1550-D (1997) D209–D244.
[33] J.C. Savage, J.L. Svarc, Postseismic deformation associated with the 1999 $m_w = 7.3$ Landers earthquake, southern California, J. Geophys. Res. 102 (1997) 7565–7577.
[34] R.E. Reilinger, S. Ergintav, R. Bürgmann, S. McClusky, O. Lenk, A. Barka, O. Gurkan, L. Hearn, K.L. Feigl, R. Cakmak, B. Aktug, H. Ozener, M.N. Töksoz, Coseismic and postseismic fault slip for the 17 August 1999, M = 7.5, Izmit, Turkey earthquake, Science 289 (2000) 1519–1524.
[35] N. Bechor, P. Segall, Y.-J. Hsu, J. McGuire, S.-B. Yu, Time-dependent inversion for post-seismic slip following the 1999 Chi-Chi Taiwan earthquake using GPS observation, EOS Trans. AGU 82 (2001) G22D-01.
[36] Y.-J. Hsu, N. Bechor, P. Segall, S.-B. Yu, L.-C. Kuo, K.-F. Ma, Rapid afterslip following the 1999 Chi-Chi, Taiwan earthquake, Geophys. Res. Lett. 29 (2002) 10.1029/2002GL014967.
[37] M.F. Linker, J.R. Rice, Models of postseismic deformation and stress transfer associated with the 1989 Loma Prieta earthquake, in: The Loma Prieta, California, Earthquake of October 17, 1989 – Postseismic Effects, Aftershocks and Other Phenomena, U.S. Geol. Surv. Prof. Pap. 1550-D (1997) D253–D275.
[38] E.H. Hearn, R. Bürgmann, R.E. Reilinger, Dynamics of Izmit earthquake postseismic deformation and loading of the Düzce earthquake hypocenter, Bull. Seism. Soc. Am. 92 (2002) 172–193.
[39] S.-I. Karato, M. Paterson, J. Fitz Gerald, Rheology of synthetic olivine aggregates: Influence of grain size and water, J. Geophys. Res. 91 (1986) 8151–8176.
[40] J.H. ter Heege, J.H.P. de Bresser, C.J. Spiers, Composite flow laws of crystalline materials with continuously distributed grain size: Theory and application to olivine, J. Struct. Geol. (2003) (submitted).
[41] M. Kameyama, D.A. Yuen, H. Fujimoto, The interaction of viscous heating with grain-size dependent rheology in the formation of localized slip zones, Geophys. Res. Lett. 24 (1997) 2523–2526.
[42] J. Braun, J. Chéry, A.N.B. Poliakov, D. Mainprice, A. Vauchez, A. Tommasi, M. Daignières, A simple parameterization of strain localization in the ductile regime due to grain size reduction: A case study for olivine, J. Geophys. Res. 104 (1999) 25167–25181.
[43] C.E. Hall, E.M. Parmentier, The influence of grain size on a convective instability, Geochem. Geophys. Geosyst. 4 (2003) 10.1029/2002GC000308.
[44] P.N. Chopra, M. Paterson, The role of water in the deformation of dunite, J. Geophys. Res. 89 (1984) 7861–7876.
[45] D. van der Wal, P. Chopra, M. Drury, J. Fitz Gerald, Relationships between dynamically recrystallized grain size and deformation conditions in experimentally deformed olivine rocks, Geophys. Res. Lett. 20 (1993) 1479–1482.
[46] G. Hirth, D.L. Kohlstedt, Rheology of the upper mantle and the mantle wedge: a view from the experimentalists,

in: J. Eiler (Ed.), The Subduction Factory, AGU Geophys. Monogr. (2002) (in press).
[47] J.H.P. de Bresser, C.J. Peach, J.P.J. Reijs, C.J. Spiers, On dynamic recrystallization during solid state flow: Effects of stress and temperature, Geophys. Res. Lett. 25 (1998) 3457–3460.
[48] J.H.P. de Bresser, J.H. ter Heege, C.J. Spiers, Grain size reduction by dynamic recrystallization: Can it result in major rheological weakening?, Int. J. Earth Sci. 90 (2001) 28–45.
[49] B. Evans, J. Renner, G. Hirth, A few remarks on the kinetics of static grain growth in rocks, Int. J. Earth Sci. 90 (2001) 88–103.
[50] J. Newman, W.M. Lamb, M.R. Drury, R.L.M. Vissers, Deformation processes in a peridotite shear zone: Reaction-softening by a H_2O-deficient, continuous net transfer reaction, Tectonophysics 303 (1999) 193–222.
[51] R.W. Hamming, Numerical Methods for Scientists and Engineers, 2nd edn., Dover, New York, 1973.
[52] C.H. Scholz, The Mechanics of Earthquakes and Faulting, 2nd edn., Cambridge University Press, New York, 2002.
[53] W.F. Brace, J.D. Byerlee, California earthquakes: Why only shallow focus?, Science 168 (1970) 1573–1575.
[54] R.M. Stesky, Mechanisms of high temperature frictional sliding in Westerly granite, Can. J. Earth Sci. 15 (1977) 362–375.
[55] S.T. Tse, J.R. Rice, Crustal earthquake instability in relation to the depth variation of frictional slip properties, J. Geophys. Res. 91 (1986) 9452–9472.
[56] D.A. Lockner, R. Summers, J.D. Byerlee, Effects of temperature and sliding rate on frictional strength of granite, Pure Appl. Geophys. 123 (1986) 445–469.
[57] F.M. Chester, A rheologic model for wet crust applied to strike-slip fault, J. Geophys. Res. 100 (1995) 13033–13044.
[58] M.L. Blanpied, C.J. Marone, D.A. Lockner, J.D. Byerlee, D.P. King, Quantitative measure of the variation in fault rheology due to fluid-rock interactions, J. Geophys. Res. 103 (1998) 9691–9712.
[59] C.J. Marone, Laboratory-derived friction law and their application to seismic faulting, Annu. Rev. Earth Planet. Sci. 26 (1998) 643–696.
[60] J.H. Dieterich, Modeling of rock friction 1: Experimental results and constitutive equations, J. Geophys. Res. 84 (1979) 2161–2168.
[61] A.L. Ruina, Slip instability and state-variable friction laws, J. Geophys. Res. 88 (1983) 10359–10370.
[62] J.R. Rice, Constitutive relations for fault slip and earthquake instabilities, Pure Appl. Geophys. 121 (1983) 443–475.
[63] J.H. Dieterich, Earthquake nucleation on faults with rate- and state-dependent strength, Tectonophysics 322 (1992) 115–134.